

Supporting Information for "No increase is detected and modeled for the seasonal cycle amplitude of $\delta^{13}\text{C}$ of atmospheric carbon dioxide"

Fortunat Joos^{1,2}, Sebastian Lienert^{1,2}, and Sönke Zaehle³

¹Climate and Environmental Physics, University of Bern, Bern Switzerland

²Oeschger Centre for Climate Change Research, University of Bern, Bern, Switzerland

³Max Planck Institute for Biogeochemistry, P.O. Box 600164, Hans-Knöll-Str. 10, 07745 Jena, Germany

Correspondence: Fortunat Joos (fortunat.joos@unibe.ch)

Contents of this file: Figures S1 to S5 and Table S1

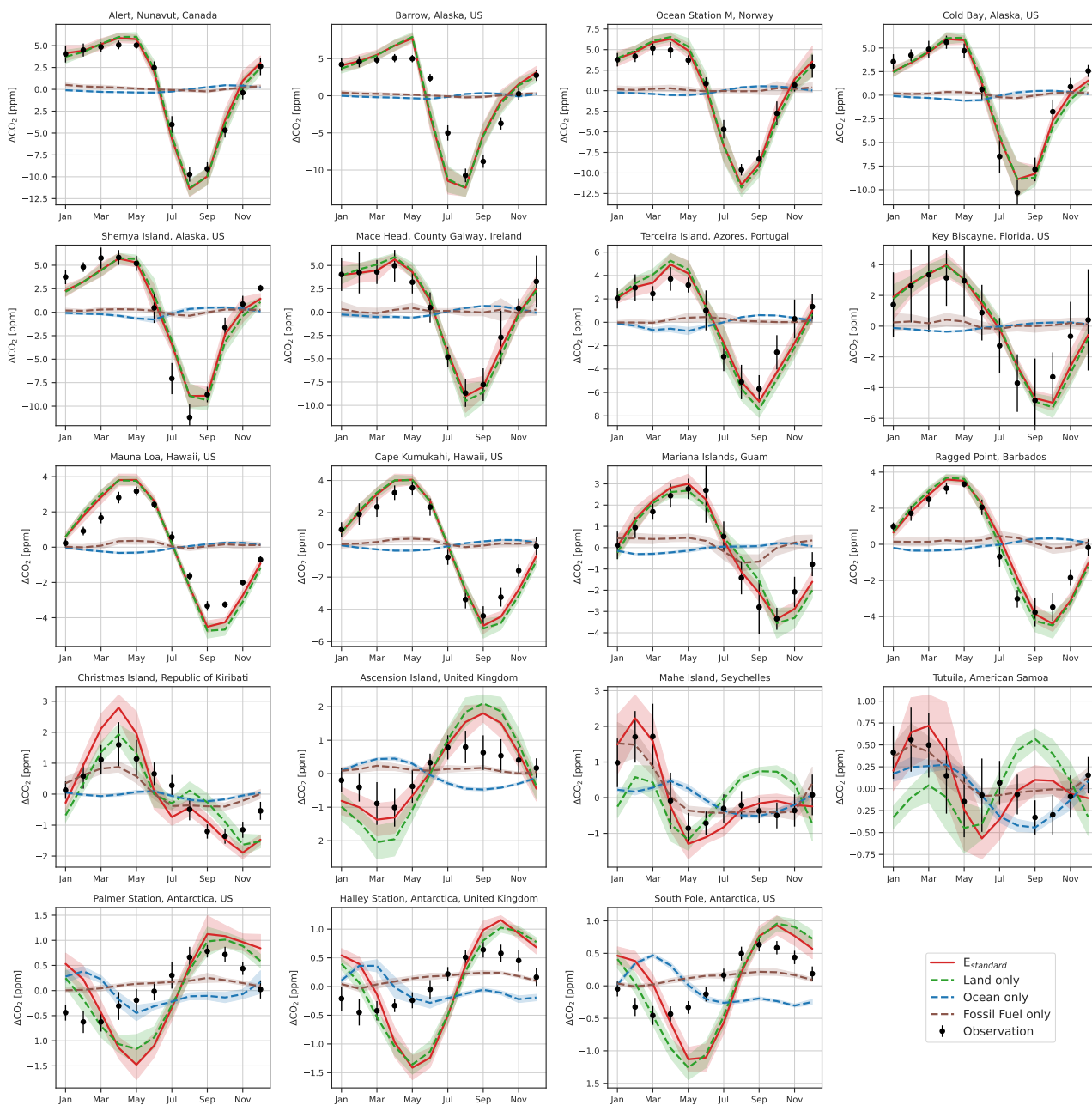


Figure S1. The seasonal cycle of CO₂ simulated by Bern3D-LPX and transported with TM3 (red), compared to observations (black dots). The calculation of the seasonal cycle only considers months between 1982 and 2012 where both the measurements and transport matrices are available. The location of the measurements is indicated in the title of the plot. The results of only transporting fluxes of terrestrial (green, dashed), oceanic (blue, dashed), and from fossil sources (brown, dashed) are shown with dashed lines. Error bars and shading correspond to the interannual standard deviation.

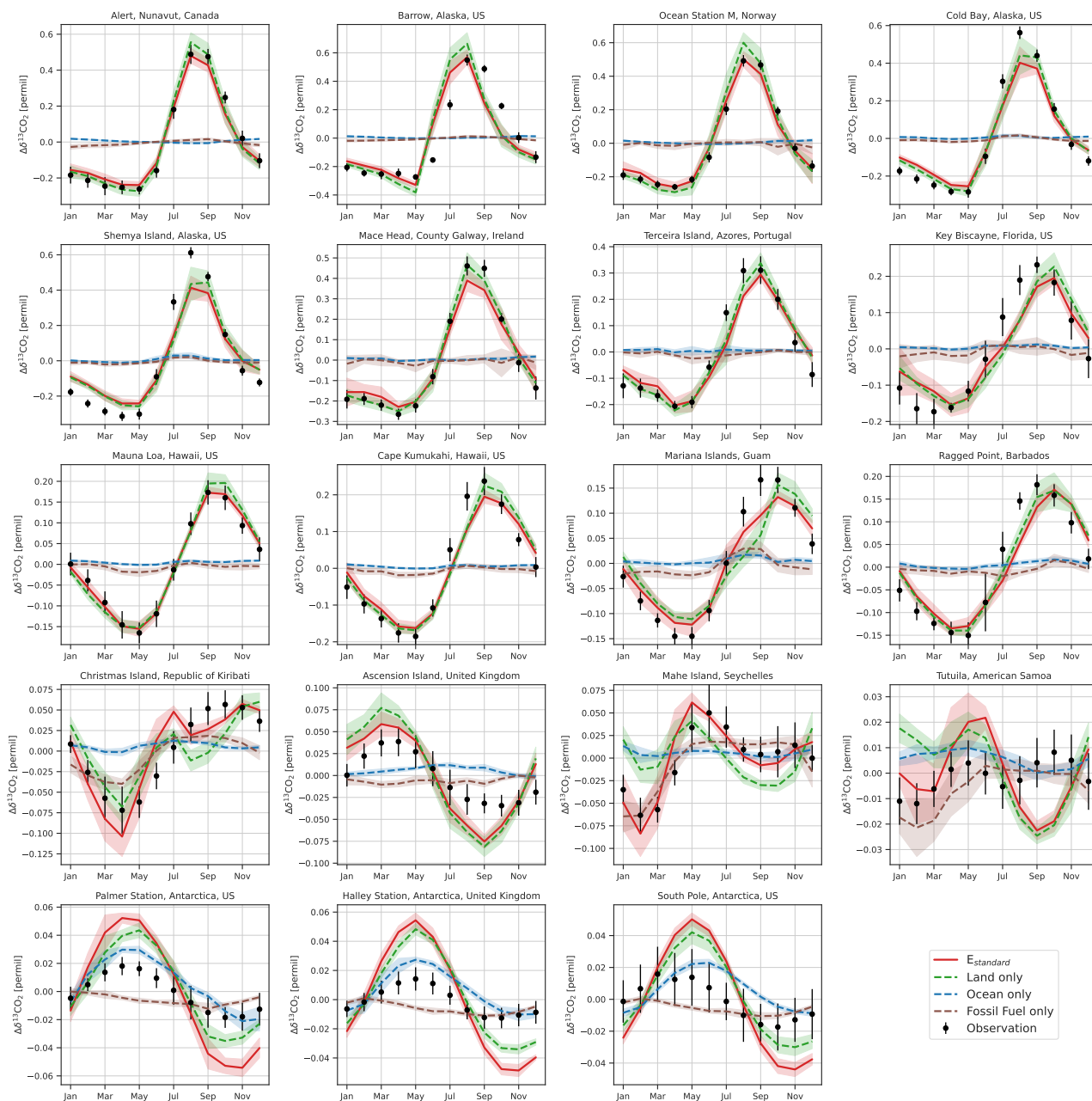


Figure S2. The seasonal cycle of $\delta^{13}\text{C}(\text{CO}_2)$ simulated by Bern3D-LPX and transported with TM3 (red), compared to observations (black dots). The calculation of the seasonal cycle only considers months between 1982 and 2012 where both the measurements and transport matrices are available. The location of the measurements is indicated in the title of the plot. The results of only transporting fluxes of terrestrial (green, dashed), oceanic (blue, dashed), and from fossil sources (brown, dashed) are shown with dashed lines. Error bars and shading correspond to the interannual standard deviation.

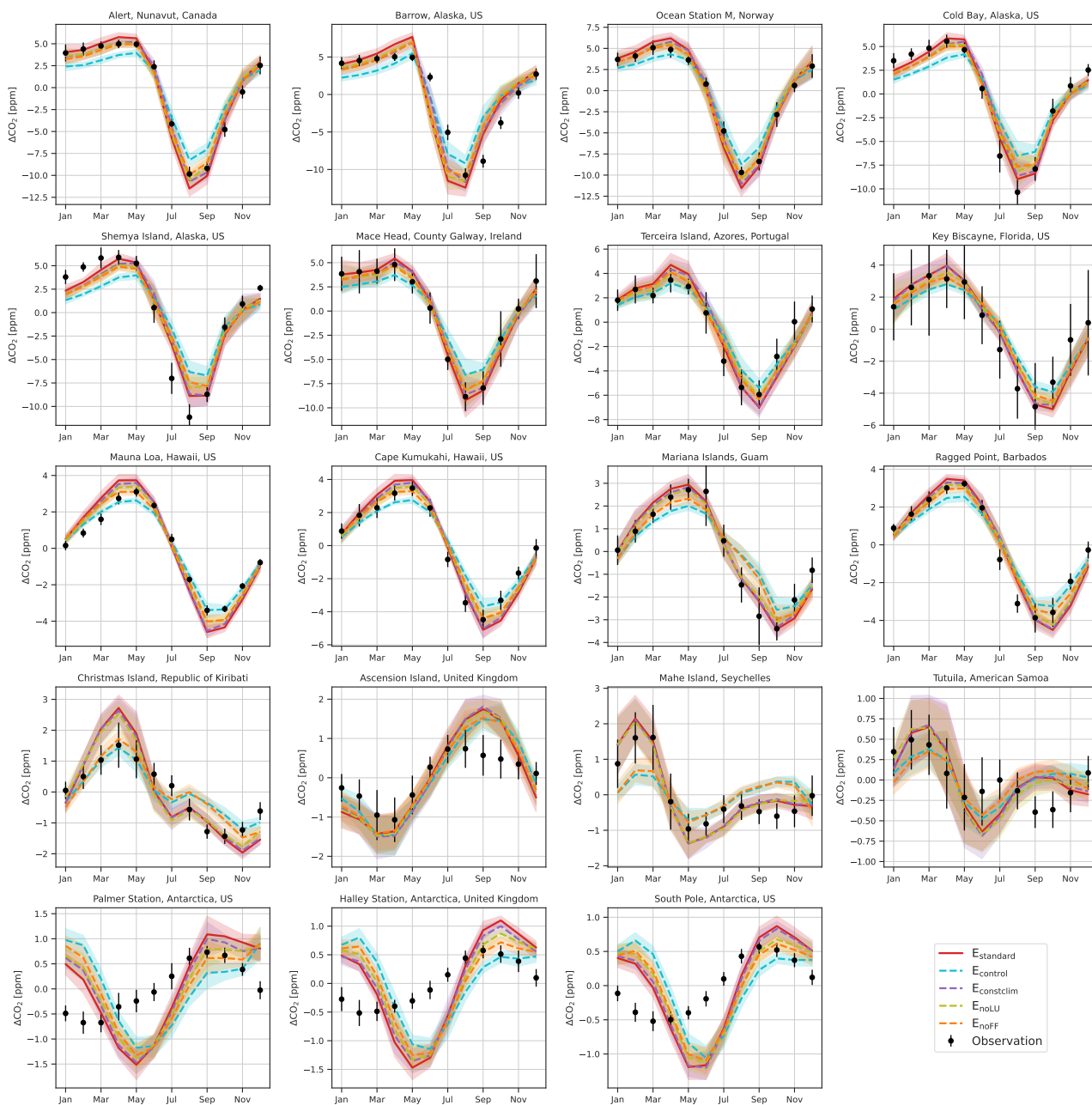


Figure S3. The seasonal cycle of CO_2 simulated by Bern3D-LPX and transported with TM3 (red), compared to observations (black dots). The calculation of the seasonal cycle only considers months between 1982 and 2012 where both the measurements and transport matrices are available. The results of sensitivity simulations are shown with dashed lines: climate ($E_{\text{constclim}}$, purple), land use area (E_{noLU} , olive), fossil fuel emissions (E_{noFF} , orange), or all forcings (E_{control} , cyan) are kept at preindustrial values. Shading and error bars correspond to the interannual standard deviation.

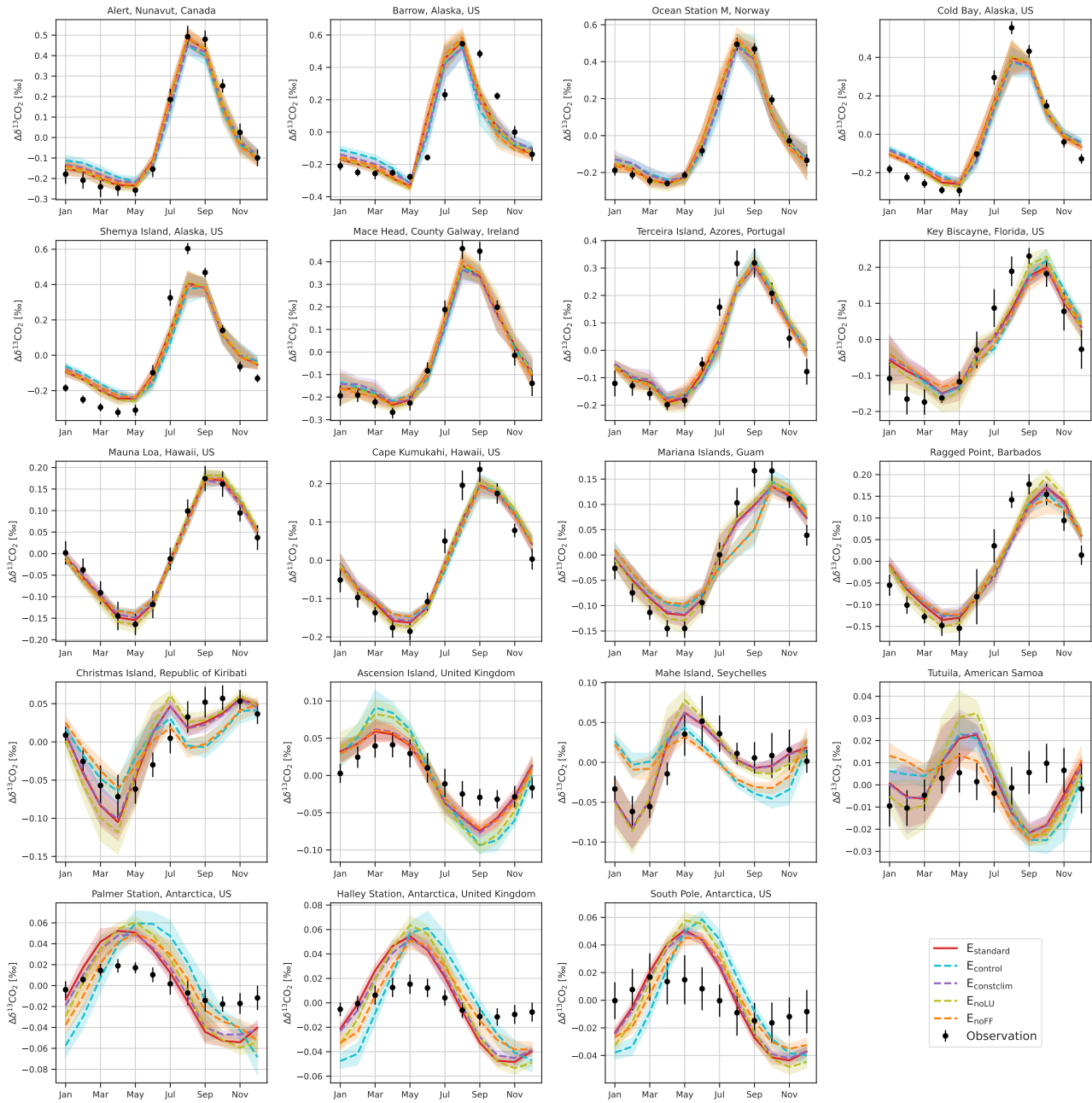


Figure S4. The seasonal cycle of $\delta^{13}\text{C}(\text{CO}_2)$ simulated by Bern3D-LPX and transported with TM3 (red), compared to observations (black dots). The calculation of the seasonal cycle only considers months between 1982 and 2012 where both the measurements and transport matrices are available. The results of sensitivity simulations are shown with dashed lines: climate ($E_{\text{constclim}}$, purple), land use area (E_{noflu} , olive), fossil fuel emissions (E_{nofff} , orange), or all forcings (E_{control} , cyan) are kept at preindustrial values. Shading and error bars correspond to the interannual standard deviation.

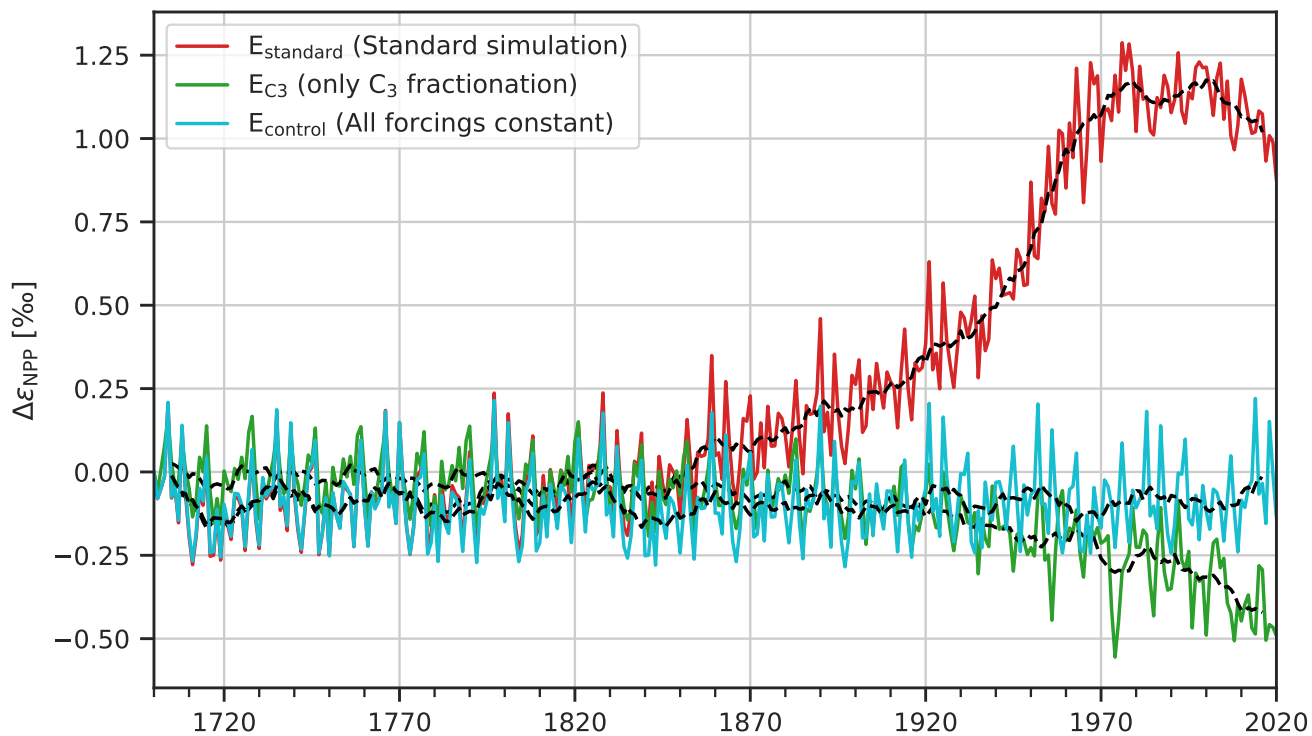


Figure S5. Simulated change in photosynthetic discrimination ϵ_{NPP} over the industrial period. The results of three simulations are shown: E_{standard} in red, E_{control} in cyan, and E_{C3} in green. In E_{C3} , the fractionation formulation for all C_4 plants is replaced by those for C_3 plants. 10-year running means are indicated with black dashed lines.

Table S1. The seasonal cycle amplitude of land isotopic fluxes, carbon fluxes, and isotopic signatures from the standard (Std; E_{standard}) and the control (Ctrl; E_{control}) simulation as summed over latitudinal bands.

	-60 to -40		-40 to -20		-20 to 0		0 to 20		20 to 40		40 to 60		60 to 80	
	Std	Ctrl	Std	Ctrl	Std	Ctrl	Std	Ctrl	Std	Ctrl	Std	Ctrl	Std	Ctrl
$\delta^{13}F_{al,net}^*$	-1.09	-0.91	-4.66	-5.06	-24.12	-27.23	-23.09	-23.67	-14.51	-12.07	-49.33	-37.73	-24.82	-19.10
$F_{al,net} \cdot \epsilon_{NPP}$	-1.15	-0.91	-3.68	-3.87	-18.42	-21.78	-17.70	-19.18	-12.77	-11.26	-49.64	-36.94	-24.31	-18.95
$R \cdot \delta_{dis}$	-0.05	0.01	-2.07	-0.98	-8.63	-5.45	-6.90	-4.46	-3.01	-1.05	-3.25	-0.79	-1.71	-0.15
Δ_{Trend}	0.11	-0.01	1.09	-0.21	2.93	-0.01	1.51	-0.03	1.27	0.24	3.57	-0.01	1.20	0.01
$(R \cdot \delta_{dis})/F_{al,net} \cdot \epsilon_{NPP}$	0.04	-0.01	0.56	0.25	0.47	0.25	0.39	0.23	0.24	0.09	0.07	0.02	0.07	0.01
	<i>Isotopic fluxes (GtC permil)</i>													
	<i>Carbon fluxes (GtC)</i>													
$F_{al,net}$	0.09	0.07	0.78	0.56	1.75	1.60	1.63	1.60	1.41	1.08	4.11	2.94	1.42	1.11
NPP	0.20	0.17	4.45	3.20	12.98	11.38	10.61	9.77	6.64	5.70	9.97	7.91	2.95	2.47
R	0.12	0.10	3.67	2.64	11.23	9.79	8.98	8.18	5.23	4.61	5.86	4.97	1.53	1.35
	<i>Isotopic signatures (permil)</i>													
ϵ_{NPP}	-13.40	-12.81	-4.69	-6.87	-10.55	-13.65	-10.85	-12.01	-9.08	-10.37	-12.09	-12.58	-17.06	-17.03
δ_{dis}	-0.40	0.09	-0.56	-0.37	-0.77	-0.56	-0.77	-0.55	-0.58	-0.23	-0.55	-0.16	-1.12	-0.11